Arch. Min. Sci. **64** (2019), 1, 3-19

Electronic version (in color) of this paper is available: http://mining.archives.pl

DOI 10.24425/ams.2018.124991

ALICJA KRZEMIEŃ*#

DYNAMIC FIRE RISK PREVENTION STRATEGY IN UNDERGROUND COAL GASIFICATION PROCESSES BY MEANS OF ARTIFICIAL NEURAL NETWORKS

DYNAMICZNA STRATEGIA ZAPOBIEGANIA RYZYKU POŻAROWEMU Z UŻYCIEM SZTUCZNYCH SIECI NEURONOWYCH W PROCESACH PODZIEMNEGO ZGAZOWANIA WĘGLA

Based on data collected during an UCG pilot-scale experiment that took place during 2014 at Wieczorek mine, an active mine located in Upper Silesia (Poland), this research focuses on developing a dynamic fire risk prevention strategy addressing underground coal gasification processes (UCG) within active mines, preventing economic and physical losses derived from fires.

To achieve this goal, the forecasting performance of two different kinds of artificial neural network models (generalized regression and multi-layer feedforward) are studied, in order to forecast the syngas temperature at the georeactor outlet with one hour of anticipation, thus giving enough time to UCG operators to adjust the amount and characteristics of the gasifying agents if necessary.

The same model could be used to avoid undesired drops in the syngas temperature, as low temperature increases precipitation of contaminants reducing the inner diameter of the return pipeline. As a consequence the whole process of UGC might be stopped. Moreover, it could allow maintaining a high temperature that will lead to an increased efficiency, as UCG is a very exothermic process.

Results of this research were compared with the ones obtained by means of Multivariate Adaptative Regression Splines (MARS), a non-parametric regression technique able to model non-linearities that cannot be adequately modelled using other regression methods.

Syngas temperature forecast with one hour of anticipation at the georeactor outlet was achieved successfully, and conclusions clearly state that generalized regression neural networks (GRNN) achieve better forecasts than multi-layer feedforward networks (MLFN) and MARS models.

Keywords: Dynamic alarm strategy, Fire risk prevention, Underground coal gasification (UCG), Generalized Regression Neural Networks (GRNN), Multi-Layer Feedforward Networks (MLFN), Multivariate Adaptative Regression Splines (MARS)

Przedstawione w niniejszej pracy badania koncentrują się na opracowaniu dynamicznej strategii zapobiegania ryzyku pożarowemu w procesach podziemnego zgazowania węgla (PZW) w czynnych kopalniach. Celem badań jest zapobieganie ekonomicznym i fizycznym stratom wynikającym z poża-

* CENTRAL MINING INSTITUTE (GIG), DEPARTMENT OF RISK ASSESSMENT AND INDUSTRIAL SAFETY, PLAC GWARKÓW 1. 40-166 KATOWICE, POLAND.

Corresponding author: akrzemien@gig.eu

rów. W pracy wykorzystano dane zebrane podczas pilotowego eksperymentu podziemnego zgazowania węgla, który odbył się w 2014 r. w czynnej Kopalni Węgla Kamiennego „Wieczorek", zlokalizowanej na Górnym Śląsku.

W artykule przeanalizowano działanie dwóch różnych modeli sztucznych sieci neuronowych, tj. sieci neuronowych realizujących uogólnione regresje GRNN oraz wielowarstwowych sieci perceptronowych MLFN, w celu prognozowania temperatury gazu syntezowego na wyjściu z georeaktora z godzinnym wyprzedzeniem. Informacja na temat temperatury na godzinę „do przodu" daje wystarczająco dużo czasu operatorowi procesu PZW na dostosowanie ilości i właściwości czynników zgazowujących do zaistniałej sytuacji.

Ten sam model można zastosować do uniknięcia niepożądanych spadków temperatury gazu syntezowego. Niska temperatura gazu sprzyja wytrącaniu się osadu (substancji smolistych), powodując zmniejszanie średnicy rurociągu odbioru gazu, co w konsekwencji może prowadzić do całkowitego zatrzymania procesu zgazowania. Model pozwala również na utrzymanie wysokiej temperatury, która prowadzi do zwiększonej wydajności procesu PZW, szczególnie biorąc pod uwagę, że PZW jest procesem bardzo egzotermicznym.

Wyniki zrealizowanych badań porównano z rezultatami uzyskanymi za pomocą modelu MARS – nieparametrycznej metody regresji zdolnej do modelowania zależność nieliniowych, których nie można odpowiednio modelować przy użyciu innych metod regresji.

Prognoza temperatury gazu na godzinę „do przodu" na wylocie georeaktora została osiągnięta z powodzeniem, a wnioski jasno pokazują, że sieci neuronowe realizujące uogólnione regresje (GRNN – Generalized Regression Neural Networks) osiągają lepsze rezultaty niż wielowarstwowe sieci jednokierunkowe (MLFN – Multi-Layer Feedforward Networks) i modele MARS (Multivariate Adaptative Regression Splines).

Słowa kluczowe: Dynamiczna strategia zapobiegania ryzyku, Prewencja ryzyka pożarowego, Podziemne zgazowanie węgla (PZW), Generalized Regression Neural Networks (GRNN), Multi-Layer Feedforward Networks (MLFN), Multivariate Adaptative Regression Splines (MARS)

1. Introduction

Hard coal resources located in protective pillars (shaft pillars, crosscut pillars, etc.) and in thin coal seems cannot be extracted in most of the cases by longwall mining methods. Also an unfavorable spatial location of coal seams, the existence of geological disturbances or a small amount of resources limit the possibility of their excavation using conventional mining exploitation methods. Those adverse conditions do not affect the use of underground coal gasification (UCG) technology.

The main advantage of UCG, apart from increasing coal resources with promising economics (Bhutto et al., 2013), is the production of gas directly where the coal is, leaving the waste underground (Białecka, 2008) and reducing the amount of preparation works during the process. The technology has also limitations, i.e. problems with process control (Burton et al., 2006), environmental hazards associated with the possibility of UCG products leakage into the surrounding strata and aquifers as well as surface deformations (Kapusta et al., 2013). Another aspect are the risks associated with the technology itself, the place of the experiment and the conditions of ground and underground infrastructure, especially in case of active hard coal mines.

UCG in an active or ready-to-abandon mine requires the application of demanding safety criteria. In first place, the process has to be controlled in order to prevent gas hazard in the ventilation galleries located in the proximity of the georeactor. Thus, to maintain a near-atmospheric pressure in the georeactor decreases the risk of toxic hazards (Wiatowski et al., 2012) as well as the pollution of groundwater by condendsed components. The location of the UCG georeactor in the zone of distress after previous longwall with caving exploitation also prevents or limits

an adequate control of the gasification process. Increased gas permeability of the rockmass surrounding the georeactor may cause uncontrolled migration of the syngas to the ventilation galleries, creating gas hazard and further causing uncontrolled flow of mine air from the ventilation galleries, creating a potencial risk of explosion in the georeactor (Krause et al., 2015).

A second aspect that has to be taken into account concerns the temperature of the syngas produced in the georeactor, as the process has to be designed in order to fulfil mining safety requirements. Although ideal temperatures for UCG were estimated by Burton et al. (2006) of being around 1,000°C, considering that it is a very exothermic process (Stańczyk et al., 2010) and that the pre-heating of the seam improves the quality of the syngas (Wang et al., 2017), the Polish State Mining Authority imposed an additional limit of 550°C regarding the maximum temperature of the syngas at the georeactor outlet, in order to prevent fire risk as well as self-ignition in case that it leaks into a gallery. Krause et al. (2015) established that self-ignition may happen when the temperature is above 600°C.

This paper will focus on developing a dynamic fire risk prevention strategy addressing underground coal gasification processes (UCG) within active mines, preventing economic and physical losses derived from fires, as dynamic alarm strategies could play an important controlling role (Zhu et al., 2016).

To achieve this goal, the forecasting performance of two different kinds of artificial neural network models (generalized regression and multi-layer perceptron) are studied, in order to forecast the syngas temperature at the georeactor outlet with one hour of anticipation, thus giving enough time to UCG operators to adjust the amount and characteristics of the gasifying agents if necessary. Results were compared with the ones obtained by Krzemień (2019) using Multivariate Adaptative Regression Splines (MARS), a non-parametric regression technique able to model non-linearities that cannot be adequately modelled using other regression methods.

2. Experimental data

This paper will analyse data obtained from an UCG pilot-scale experiment that took place during 2014 at Wieczorek mine, an active mine located in Upper Silesia (Poland). The UCG process was developed during 60 days, addressing coal seam nº 501, with a thickness of 5.4 m and located 460 m deep. Its theoretical gasifying capacity was of 600 kg/h of coal (maximum) with a lower calorific value of 28.9 MJ/kg, and an equivalent gas contained enthalpy of around 3 MW (Mocek et al., 2016).

The UCG process was conducted with low-pressure method. Georeactor was located close to the shaft and keeping some distance from the zone of distress after previous longwall with caving exploitation in order to minimize the risk of uncontrolled gas migration. Three channels were drilled in order to supply gasifying agents, to collect the produced syngas, to supply inertization agent and to remove the excess of water during the drilling operations (Fig. 1).

The supply channel and the production channel were drilled from the experimental gallery at the level of 400 m, while the third channel was drilled from the incline transporting drift in coal seam 510. The distance of the experimental gallery to coal seam 501 was of 2.6 m.

The main aim of the experiment was to analyse the behaviour of the process by using alternative gasifying agents: air, oxygen-enriched air and air combined with CO_2, N_2 or water. The volume and temperature of the syngas as well as its dry composition after cleaning were measured at the outlet of the georeactor on an hourly basis. Also the pressure of the syngas was

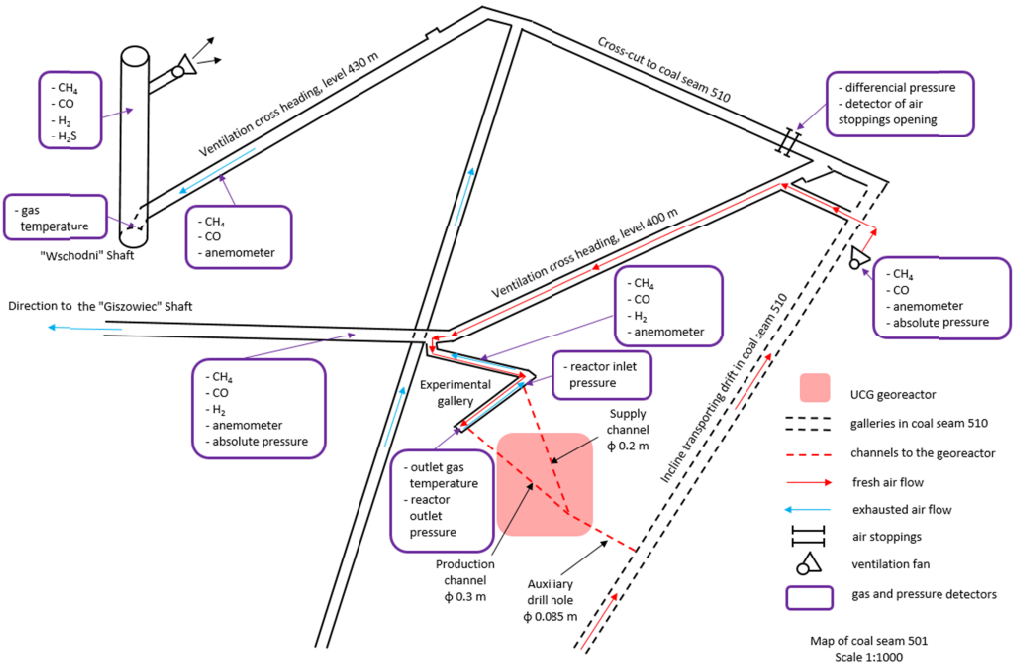

Fig. 1. UCG georeactor scheme

measured but, as only a limited amount of measures was available, it was not possible to consider this variable within the model.

Table 1 presents the variables used in the model, their units as well as the names given for developing the study.

The different phases of the experiment are presented in Figure 2, comprising more than 1,300 hours including the cooling down. Phase I started by igniting with a pyrotechnic charge the georeactor, using as gasifying agent oxygen-enriched air. Phase II consisted in gasifying only with air, although in specific moments water was also used in order to analyse the behaviour of the reactor. During this phase a technological downtime occurred, due to problems in one of the separators related with high levels of condensation. Phase III used air and carbon dioxide as gasifying agents, allowing to test the influence of carbon dioxide. Phase IV used again only air as gasifying agent, in order to re-heat the process after the descend of temperature caused by the use of carbon dioxide in the previous phase. Phase V used a decreasing amount of air and an increasing amount of nitrogen in order to start extinguishing the experiment. Finally, and with the use of nitrogen, the experiment was cooled down. This final stage was not considered within the analysis.

Table 2 presents the linear correlations among all the variables used in the model.

The temperature of the syngas (Temp_out) has a significant positive correlation with the amount of air (air_in), something reasonable as it was the main gasifying agent used. Moreover, this correlation is congruent with the most exothermic reactions within a gasification process (Wiatowski et al., 2016). It also has significant positive correlation with the amount of CH_4 (CH_4_out) produced during the gasification process, followed by the syngas volume (flow).

TABLE 1

Variables used in the model

Gasifying agents	Variable name	Units
Air	air_in	Nm^3/h
O_2	O_2_in	Nm^3/h
CO_2	CO_2_in	Nm^3/h
N_2	N_2_in	Nm^3/h
H_2O	H_2O_in	Nm^3/h
Syngas		
Temperature	Temp_out	°C
Volume	flow	Nm^3/h
Calorific value	cal	MJ/Nm^3
Dry syngas composition after cleaning		
O_2	O_2_out	%vol.
CO_2	CO_2_out	%vol.
CO	CO_out	%vol.
CH_4	CH_4_out	%vol.
H_2	H_2_out	%vol.
N_2	N_2_out	%vol.

Fig. 2. Temperature of the syngas and amounts of gasifying agents in Nm^3/h used during the UCG process during the different phases of the experiment

TABLE 2

Linear correlations of the variables used in the model

	air_in	N_2_ in	CO_2_ in	O_2_ in	H_2O_ in	O_2_ out	CO_2_ out	CO_ out	CH_4_ out	H_2_ out	N_2_ out	flow	cal	TEMP_ out
air_in	1.000	–0.363	0.076	–0.041	0.049	–0.397	0.306	–0.032	**0.537**	–0.392	–0.395	**0.644**	–0.272	**0.648**
N_2_in	–0.363	1.000	–0.097	–0.107	–0.071	–0.051	0.275	–0.268	–0.240	–0.110	–0.155	–0.254	–0.279	–0.108
CO_2_in	0.076	–0.097	1.000	–0.098	–0.065	–0.033	–0.017	**0.569**	0.149	–0.099	–0.162	0.175	–0.096	0.030
O_2_in	–0.041	–0.107	–0.098	1.000	–0.072	–0.036	**–0.634**	0.393	–0.449	**0.647**	**0.642**	0.031	0.157	–0.311
H_2O_in	0.049	–0.071	–0.065	–0.072	1.000	–0.046	0.023	0.073	0.104	–0.110	–0.041	0.054	–0.043	0.067
O_2_out	–0.397	–0.051	–0.033	–0.036	–0.046	1.000	–0.052	–0.147	–0.229	0.095	0.073	–0.475	0.232	–0.470
CO_2_out	0.306	0.275	–0.017	**–0.634**	0.023	–0.052	1.000	**–0.646**	**0.546**	**–0.941**	**–0.964**	0.015	**–0.556**	0.366
CO_out	–0.032	–0.268	**0.569**	0.393	0.073	–0.147	**–0.646**	1.000	–0.333	**0.520**	0.492	0.207	0.046	–0.154
CH_4_out	**0.537**	–0.240	0.149	–0.449	0.104	–0.229	**0.546**	–0.333	1.000	**–0.730**	**–0.675**	0.368	0.089	**0.527**
H_2_out	–0.392	–0.110	–0.099	**0.647**	–0.110	0.095	**–0.941**	**0.520**	**–0.730**	1.000	**0.964**	–0.125	0.454	–0.422
N_2_out	–0.395	–0.155	–0.162	**0.642**	–0.041	0.073	**–0.964**	0.492	**–0.675**	**0.964**	1.000	–0.112	0.498	–0.417
flow	**0.644**	–0.254	0.175	0.031	0.054	–0.475	0.015	0.207	0.368	–0.125	–0.112	1.000	–0.224	0.495
cal	–0.272	–0.279	–0.096	0.157	–0.043	0.232	**–0.556**	0.046	0.089	0.454	0.498	–0.224	1.000	–0.289
TEMP_ out	0.648	–0.108	0.030	–0.311	0.067	–0.470	0.366	–0.154	**0.527**	–0.422	–0.417	0.495	–0.289	1.000

Figures in bold represent all the correlations greater than |0.5|

Regarding the calorific value of the syngas (cal), the biggest positive correlations are with the amount of N_2 (N_2_out) and H_2 (H_2_out) produced during the gasification.

3. Methodology

During this research two types of artificial neural network models were used in order to develop a dynamic alarm strategy addressing fire risk prevention: Generalized Regression Neural Networks (GRNN) and Multi-Layer Feedforward Networks (MLFN), also referred to as Multi-Layer Perceptron Networks (MLPN), with one or two hidden layers. The tool that was used to develop the neural network models is NeuralTools 7.5, from Palisade Corporation (Ithaca, New York).

GRNN are very close to probabilistic neural networks (PNN). GRNN are used for predicting numerical functions, while PNN are used for predicting categories and classification. Both of them were presented by Specht (1991). In these artificial neural networks, the prediction of an unknown dependent value is achieved interpolating training cases, giving more weight to neighbouring cases. During the training, the optimal interpolation parameters are determined. One big advantage of these neural networks is that there is no need to configurate them at all.

Figure 3 presents a GRNN with four independent numeric variables. The pattern layer contains one node for each training case, assuming in this case that there are just four training cases.

The presentation of a training case in this network consists in presenting four independent numerical values. Each neuron in the pattern layer calculates its distance from the case presented. The values transferred to the summation layer (numerator and denominator node) are functions of both distance and the dependent value: the two nodes add up their input values, while the exit node divides them to generate the prediction.

The distance functions that are computed in the pattern layer use "smoothing factors", having every input its own value. The greater the value of the smoothing factor, the more significant distant training cases become for the predicted value. With multiple inputs, the smoothing factor relates to the distance along one dimension in multi-dimensional space.

On the other hand, a Multi-Layer Feedforward Network (MLFN) is a feedforward neural network model that maps different sets of input data into an appropriate output set. They are a variation of the standard linear perceptron (Sánchez Lasheras et al., 2010). The MLFN architecture consists in one input layer of neurons, one or two hidden layers of neurons and an output layer. They are able to approximate complex relationships between independent variables and a dependent variable.

Figure 4 shows a MLFN with the following topology: four independent variables in the input layer, one dependent variable in the output layer, two nodes in the first hidden layer and three nodes in the second hidden layer. Nevertheless, to achieve a better prediction accuracy, the second hidden layer is hardly ever needed.

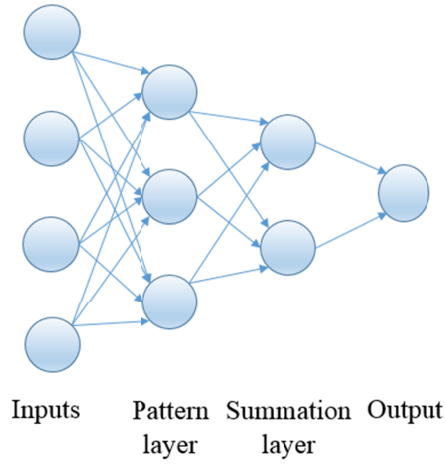

Fig. 3. Generalized Regression Neural Network (GRNN) with three training cases in the pattern layer and four independent numeric variables in the input layer

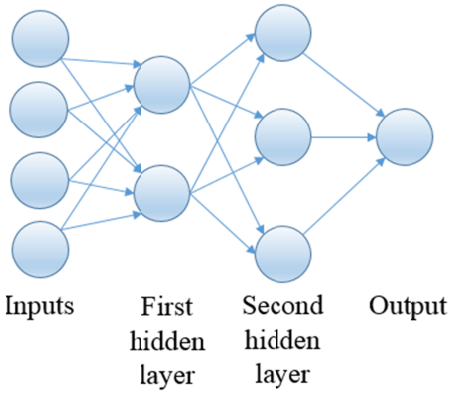

Fig. 4. Multi-Layer Feedforward Network with four independent numeric variables in the input layer

Nowadays, MLFN using a backpropagation algorithm can be considered as a standard algorithm for supervised learning pattern recognition. In a MLFN the learning takes place by means of connection weight changes after processing each piece of data, based on a comparison between the amount of error and the expected result. The behaviour of the net is determined by the topology, a parameter assigned to each connection (weight) and a parameter assigned to each node (bias term), plus an activation function that is used to convert the inputs of each node into an output.

A sigmoid function, specifically a hyperbolic tangent function in the case of NeuralTools 7.5, is used as activation function within hidden layer nodes, returning the output node the weighted sum of the inputs.

In order to determine the optimum topology of a MLFN, mainly focused on calculating the amount of neurons in hidden layers, there are two alternatives: to undergo a design of experi-

ments (DOE) or to undergo a best net search by testing randomly selected cases. The last one will be used in this research.

After determining which artificial neural network model fits the best the UCG process, its results will be compared with the ones obtained by Krzemień (2019), who used a Multivariate Adaptative Regression Splines (MARS) model, a supervised learning predictive technique of artificial intelligence that uses non-parametric regression techniques able to model non-linearities that cannot be adequately modelled using other regression methods, and that were firstly introduced by Friedman (1991). This model was developed by means of the R language (R Core Team, 2017) with the EARTH package (Milborrow, 2017).

In order to compare both models (neural networks and MARS model), the percentile 95 of the absolute differences between real values and forecasts will be used. Also, the importance of the variables that take part in both models will be analysed. In the case of the MARS models, the estimated importance of the basis functions is established by means of the generalized cross-validation (GCV), that counting for each variable the number of subsets n or $n_{subsets}$, calculates the residual sum of squares (RSS) divided by a smoothing parameter or a penalty depending on the model complexity (Sekulic & Kowalski, 1992; Álvarez Antón et al., 2013; Menéndez Álvarez et al., 2017):

$$GCV\left(M\right)=\frac{RSS/n}{\left(1-C\left(M\right)/n\right)^{2}} \tag{1}$$

where:

$$RSS=\sum_{i=1}^{n}\left(y_i-\hat{f}_M\left(\hat{x}_i\right)\right)^{2} \tag{2}$$

and:

$$C\left(M\right)=\left(M+1\right)+d\times M \tag{3}$$

being y the dependent continuous variable, $\hat{f}_M(\vec{x})$ the expression of the MARS model, M the number of basis functions and d the penalty for each basis function.

4. Discussion

In first place, a best net search was developed by testing randomly selected cases using GRNN and MLFN with 2 to 6 nodes in the first hidden layer. As it was said before, the second hidden layer is hardly ever needed to achieve better prediction accuracy, thus it was not considered in the research. For the training an aleatory 80% of the data set was used, while the remaining 20% was used for testing. Training and testing results are shown in Table 3.

Although the MLFN with 4 nodes achieved the best testing results, as GRNN training results were much better, both nets were trained using the 100% of the data set. Finally, GRNN was selected as 10% tolerance, the root mean square error (RMSE), the mean absolute error (MAE) as well as the standard deviation of absolute error were much lower than in the MLFN with 4 nodes in the first hidden layer.

Figure 5 shows the scatterplot of predicted versus actual values of the syngas temperature and Figure 6 shows the histogram of residuals obtained in the training of the GRNN.

TABLE 3

Training and testing results of the different neural network configurations

Configuration	GRNN	MLFN (2 nodes)	MLFN (3 nodes)	MLFN (4 nodes)	MLFN (5 nodes)	MLFN (6 nodes)
Training						
Number of Cases	987	987	987	987	987	987
% Bad Predictions (10% Tolerance)	0.2026%	1.0132%	0.9119%	0.8105%	0.9119%	0.9119%
Root Mean Square Error	4.173	9.201	9.095	8.912	8.986	9.445
Mean Absolute Error	1.769	4.154	4.674	4.107	4.296	5.025
Std. Deviation of Abs. Error	3.780	8.210	7.802	7.910	7.892	7.997
Testing						
Number of Cases	247	247	247	247	247	247
% Bad Predictions (10% Tolerance)	2.4291%	1.2146%	1.2146%	0.4049%	0.8097%	0.4049%
Root Mean Square Error	8.536	7.876	9.462	6.359	6.362	7.702
Mean Absolute Error	4.469	4.263	5.282	4.177	4.136	5.270
Std. Deviation of Abs. Error	7.272	6.622	7.850	4.795	4.835	5.616

Coloured figures represent the best training results that were achieved

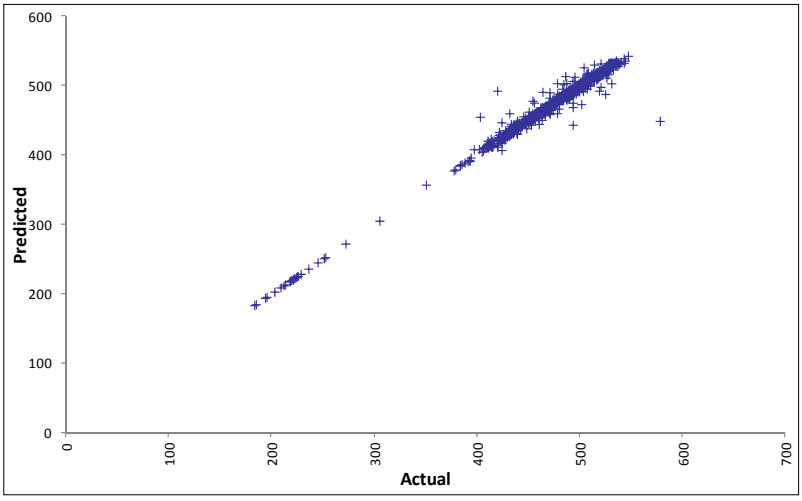

Fig. 5. Predicted versus actual values of the syngas temperature in the training of the GRNN

The GRNN model calculates the temperature for the next hour in the 95% of the cases with a difference of less than 9°C (Table 4). On the other hand, the MARS model was able to forecast the temperature in the 95% of the cases with a difference of less than 15°C (Krzemień, 2019). Thus, the superiority of the GRNN model can be stated. It has to be remarked that 9°C represents less than 2% of 550°C, which was the temperature limit imposed in order to prevent fires within the mine.

Table 5 presents a comparison of the relative variable impacts from both models is presented.

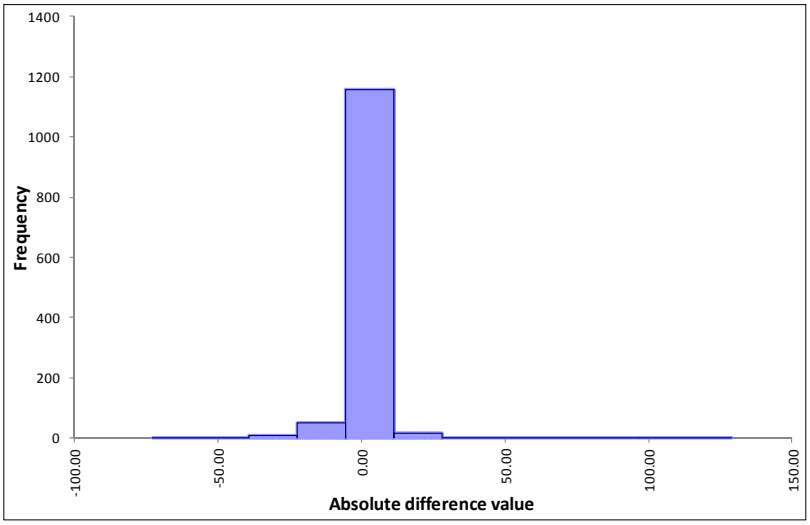

Fig. 6. Histogram of residuals in the training of the GRNN

TABLE 4

Percentiles of the absolute differences of real values and forecasts for all the phases of the experiment

Phase	10%	20%	80%	90%	95%	**99%**
All	0.2	0.6	3.8	5.7	**8.4**	24.4
I	0.5	0.9	3.8	5.6	**9.0**	13.8
II	0.0	0.1	2.3	3.6	**5.1**	18.4
III	0.0	0.0	0.0	0.2	**0.3**	1.4
IV	0.2	0.4	2.9	4.5	**6.7**	19.1
V	0.1	0.4	3.6	4.6	**6.2**	14.8

Apart from the Temperature (Temp_out) of the syngas, the two most relevant variables for the GRNN model are the amount of N_2 (N_2_in) used as gasifying agent, followed closely by the percentage of O_2 in the syngas (O_2_out). In the case of the MARS model the two most relevant variables are, at the same level, the percentage of O_2 in the syngas (O_2_out) and the syngas flow (flow).

The fact that the percentage of O_2 in the syngas (O_2_out) has such a relevance was demonstrated by Kačur & Kostúr (2017), that claimed to have solved the UCG process control by means of stabilizing both the temperature and the concentration of O_2 in the syngas. On the other hand, the syngas flow (flow) is very relevant for the MARS model as it does not use all the different gasifying agents but N_2 (N_2_in), while for GRNN model is almost irrelevant, as it uses all the gasifying agents.

In order to test the robustness of the GRNN model, five re-trainings were developed using an aleatory 80% of the data as a training subset, and the remaining 20% as a validation subset. Table 6 present the percentiles of absolute differences of real versus forecasted values in the five repetitions. In all of them, temperature is predicted in the 95% of cases with a difference of less than 11°C. Thus, the model can be considered robust.

TABLE 5

Relative variable impacts for the GRNN model and for the MARS model (Krzemień, 2019) for the whole experiment

Variable	GRNN	$n_{subsets}$	RSS	GCV
Temp_out	46.8%	17	100.0	100.0
O_2_out	10.5%	14	7.5	7.1
Flow	0.0%	14	7.5	7.1
CH_4_out	0.6%	14	7.3	6.8
H_2_out	0.3%	13	6.7	6.2
N_2_in	10.7%	12	5.5	5.0
Cal	4.2%	11	5.3	4.8
N_2_out	3.5%	7	3.6	3.0
CO_out	2.9%	5	2.6	2.0
CO_2 out	7.9%	—	—	—
H_2O_in	5.5%	—	—	—
O_2_in	4.5%	—	—	—
CO_2_in	2.6%	—	—	—
Air_in	0.3%	—	—	—

TABLE 6

Percentiles of absolute differences of real versus forecasted values in the five re-trainings

	10%	20%	80%	90%	95%	99%
1st re-training	0.2	0.5	3.3	5.2	**10.8**	27.3
2nd re-training	0.2	0.5	3.3	5.2	**8.2**	25.7
3rd re-training	0.1	0.4	3.2	5.4	**8.8**	27.7
4th re-training	0.2	0.4	3.1	5.0	**8.4**	25.6
5th re-training	0.1	0.3	3.0	4.8	**8.3**	21.1

Analysing now the different phases of the experiment separately and, starting by Phase I, a best net search was developed again. Table 7 shows the training results in terms of RMSE, achieving the GRNN the best result.

TABLE 7

Training results of the different neural network configurations for Phase I

Configuration	RMSE
GRNN	5.14
MLFN 2 Nodes	5.80
MLFN 3 Nodes	5.51
MLFN 4 Nodes	10.29
MLFN 5 Nodes	7.48
MLFN 6 Nodes	6.11

Building a GRNN model only for Phase I where oxygen-enriched air was the gasifying agent, the model is able to predict temperature values of one hour ahead with a difference of less

than 9°C in the 95% of cases (Table 4). In the case of the MARS model (Krzemień, 2019), it was able to predict the temperature values with a difference of less than 11°C in the 95% of cases.

Figure 7 presents the importance of the variables that took part in the GRNN model of Phase I. The GRNN model uses all the variables (eleven, as N_2, CO_2 and H_2O are not used as gasifying agents during this phase) while the MARS model (Krzemień, 2019) uses only eight terms, achieving quite a similar result although a little less accurate.

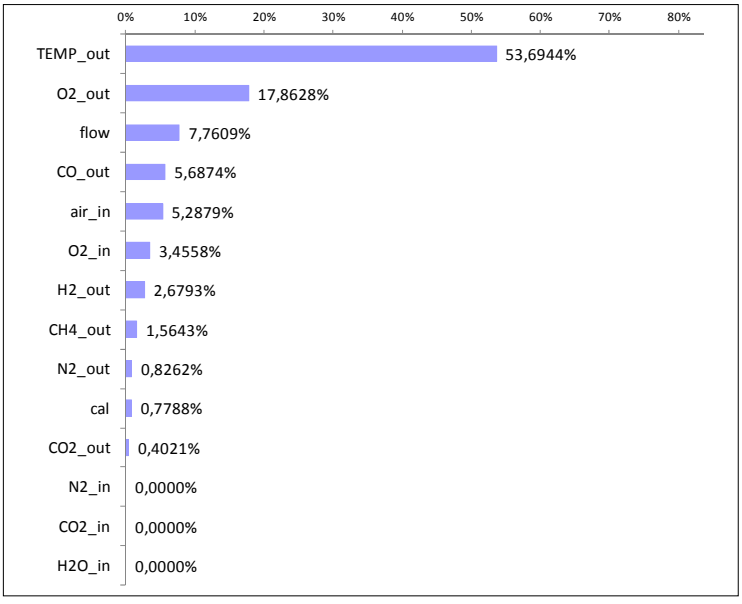

Fig. 7. Relative variable impacts that take part in the GRNN model for Phase I

Again, the percentage of O_2 in the syngas (O_2_out) is the most important variable after the temperature of the syngas (Temp_out) for the GRNN, in line with Kačur & Kostúr (2017), while for the MARS model (Krzemień, 2019) the amount of O_2 in the gasifying agent (O_2_in) and the percentage of CH_4 in the syngas (CH_4_out) are the most important variables.

Addressing now Phase II which used air as the main gasifying agent (although in specific moments water was also used, as well as O_2 and N_2), the GRNN model is able to forecast the temperature in the 95% of cases with a difference of less than 6°C (Table 4), while the MARS model (Krzemień, 2019) predicted the temperature in the 95% of cases with a difference of less than 19°C. During this phase a technological downtime occurred, due to problems in one of the separators related with high levels of condensation. Figure 8 presents the importance of the variables that took part in the GRNN model of Phase II.

In Phase III, that used as gasifying agents air and CO_2, the GRNN model was able to predict temperature in the 95% of cases with a difference of less than 1°C (Table 4), while the MARS model (Krzemień, 2019) achieved in the 95% of cases a difference of less than 5°C. Figure 9 presents the importance of the variables that took part in the GRNN model of Phase III.

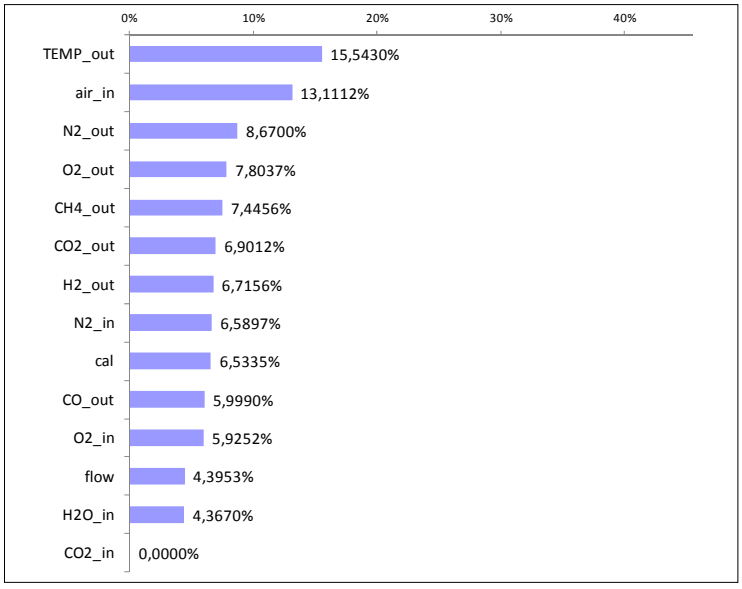

Fig. 8. Relative variable impacts that take part in the GRNN model for Phase II

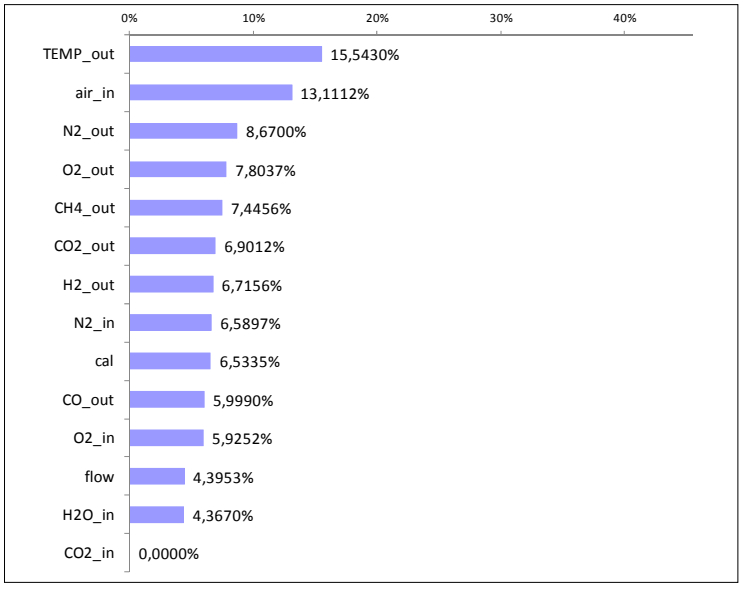

Fig. 9. Relative variable impacts that take part in the GRNN model for Phase III

In Phase IV, that used only air as gasifying agent in order to reheat the georeactor after the CO_2 stage, the GRNN model was able to forecast the temperature in the 95% of cases with a difference of less than 7°C (Table 4). The MARS model (Krzemień, 2019) was able to forecast

the temperatures in the 95% of cases with a difference of less than 8°C. Figure 10 presents the importance of the variables that took part in the GRNN model for Phase IV.

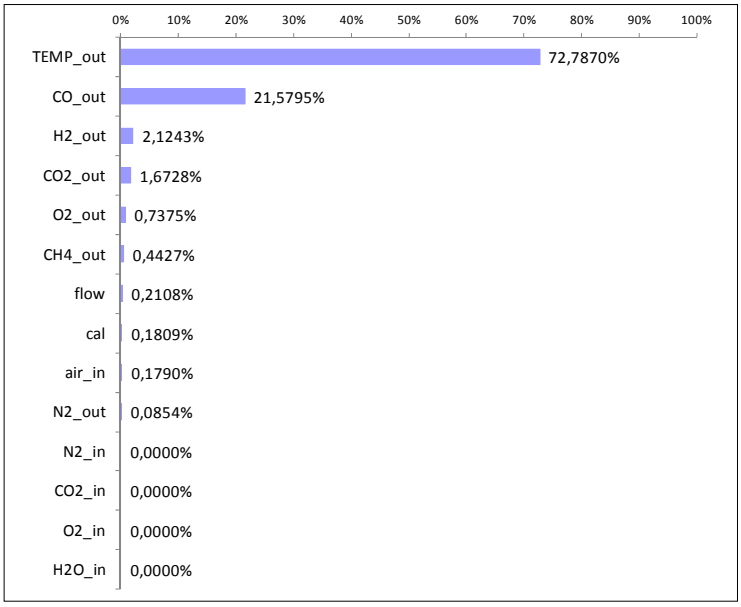

Fig. 10. Relative variable impacts that take part in the GRNN model for Phase IV

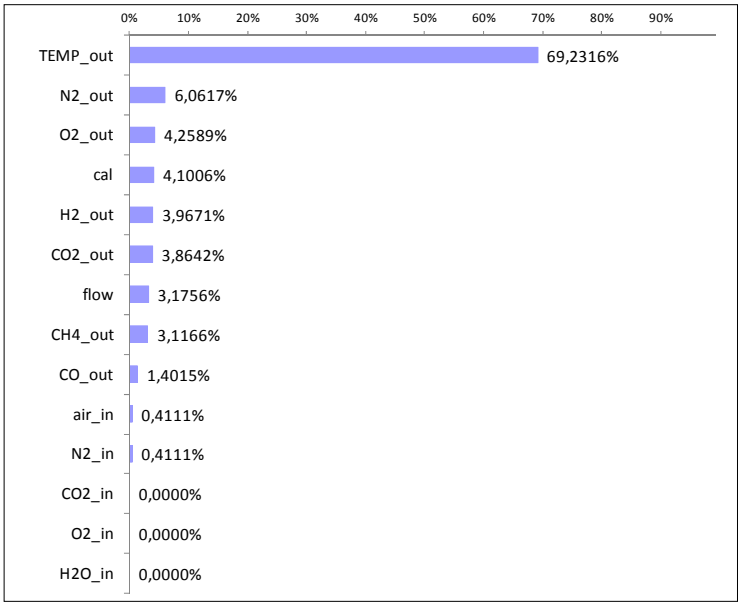

Fig. 11. Relative variable impacts that take part in the GRNN model for Phase V

In this case, the GRNN model uses only one variable more than the MARS model (Krzemień, 2019): the volume of syngas (flow), that has a relative impact of only 0.2%. This can explain the fact that both forecasts have very similar values. Moreover, the difference between the forecasts (1°C) is equal to the 0.2% of the maximum temperature (550°C).

Phase V used air and N_2 as gasifying agents to start extinguishing the georeactor. The GRNN model forecast the temperature in the 95% of cases with a difference of less than 7°C (Table 4), while the MARS model (Krzemień, 2019) was able to forecast the temperature in the 95% of cases with a difference less than 11°C. Figure 11 shows the importance of the variables that took part in the GRNN model of Phase V.

Finally, Table 8 presents a comparison between GRNN and MARS models' results for the whole experiment as well as for its different phases. In all the cases GRNN models are superior to MARS models, and use a larger amount of variables as well. The smaller the difference between the number of variables used by both methods, the lower the difference between the forecasts. Nevertheless, in case of Phase II the bigger difference may have been caused because of the technical downtime that occurred during this phase.

TABLE 8

Percentile 95 of the absolute differences of real values and forecasts for the GRNN models and for the MARS models (Krzemień, 2019) and the number of variables used by each model

Phase	GRNN		MARS	
	Percentile 95%	nº of variables	Percentile 95%	nº of variables
All	9ºC	14	15ºC	9
I	9ºC	11	11ºC	8
II	6ºC	13	19ºC	8
III	1ºC	11	5ºC	6
IV	7ºC	10	8ºC	9
V	7ºC	11	11ºC	6

5. Conclusions

This paper focuses on developing a dynamic alarm strategy addressing fire risk prevention within UCG processes using data obtained from a pilot-scale experiment that took place during 2014 at Wieczorek mine, an active mine located in Upper Silesia (Poland).

To achieve this goal, artificial neural network models were developed addressing the feasibility of forecasting the temperature of the syngas with one hour of anticipation. Two different kinds of artificial neural networks were analysed: GRNN and MLFN.

GRNN model gives more accurate forecasts of the syngas temperature than the different MLFN models tested. GRNN model was able to predict the temperature of one hour ahead in the 95% of the cases with an error less than a 2% of the maximum temperature allowed by the Mining Authority in order to prevent within an active mine the risk of fires (550°C).

Results were compared with the ones obtained by Krzemień (2019) while analysing the same data using a MARS model. GRNN model prediction was more accurate (9°C against 15°C in the 95% of cases), thus demonstrating its superiority. While the GRNN model used all the variables involved in the experiment, the number of variables used by the MARS model was lower and,

subsequently, achieved a worst prediction. Nevertheless, while neural networks achieve their results through a process that is a 'black box' for the user, MARS models present the advantage that results are expressed as a formula. Thus, it is possible to understand how the model undergoes calculations, something that could be of interest in some cases.

The study also set the significance of the variables involved within the GRNN model. After the syngas temperature, the amount of N_2 used as gasifying agent was the most important variable, followed very closely by the percentage of O_2 in the syngas. As the N_2 was only used for extinguishing the georeactor, these results are in line with the relevance of the percentage of O_2 in the syngas that was demonstrated by Kačur & Kostúr (2017), who claimed to have solved the UCG process control by means of stabilizing both the temperature and the concentration of O_2 in the syngas.

After these results, the GRNN technique was applied to the different phases of the experiment on an individual basis. A better forecast was obtained in all of the phases, improving always results given by the MARS models.

Summarizing, GRNN models can predict with high precision the interaction between the different UCG process parameters. Thus, they allow developing a sound dynamic fire risk prevention strategy, even with a limited amount of measures. This aspect is critical for the economic and technical success of UCG as the higher the temperature, the better the efficiency of the whole process. The same model could be used to avoid undesired drops in the syngas temperature, as low temperature increases precipitation of contaminants reducing the inner diameter of the return pipeline. As a consequence the whole process of UGC might be stopped (Dubiński & Turek, 2015).

Finally and as stated in Krzemień (2019), a period of five days is considered appropriate in order to develop a new GRNN model, as it is coincident with the duration of the phase that had the smallest duration in the experiment and which allowed to train a GRNN model on its own.

Acknowledgements

This work was performed as part of the project titled "Elaboration of coal gasification technology for a high efficiency production of fuels and electricity", supported by the National Centre for Research and Development in Poland, under the contract nº. SP/E/3/7708/10.

References

Álvarez Antón J.C., García Nieto P.J., de Cos Juez F.J., Sánchez Lasheras F., Viejo C.B., Roqueñí Gutiérrez N., 2013. *Battery State-of-Charge Estimator Using the MARS Technique*. IEEE Transactions on Power Electronics **28** (8), 3798-3805. https://doi.org/10.1109/TPEL.2012.2230026

Bhutto A.W., Bazmi A.A. Zahedi G., 2013. *Underground coal gasification: From fundamentals to applications*. Progress in Energy and Combustion Science **39** (1), 189-214. https://doi.org/10.1016/j.pecs.2012.09.004

Białecka B., 2008. *Estimation of coal reserves for UCG in the upper silesian coal Basin, Poland*. Natural Resources Research **17(**1), 21-28. https://doi.org/10.1007/s11053-008-9061-1

Burton E., Friedmann J., Upadhye R., 2006. *Best Practices in Underground Coal Gasification*. U.S. Department of Energy, Contract No. W-7405-Eng-48. Lawrence Livermore National Laboratory, Livermore, CA.

Dubiński J., Turek M., 2015. *Basic Aspects of Productivity of Underground Coal Gasification Process*. Archives of Mining Sciences **60** (2), 443-453. https://doi.org/10.1515/amsc-2015-0029

Friedman J.H., 1991. *Multivariate Adaptive Regression Splines*. The Annals of Statistics **19** (1), 1-67. https://doi.org/10.1214/aos/1176347963

Kačur J., Kostúr K., 2017. *Approaches to the gas control in UCG*. Acta Polytechnica **57** (3), 182-200. https://doi.org/10.14311/AP.2017.57.0182

Kapusta K., Stańczyk K., Wiatowski M., Chećko J., 2013. *Environmental aspects of a field-scale underground coal gasification trial in a shallow coal seam at the Experimental Mine Barbara in Poland*. Fuel **113 (**0), 196-208. https://doi.org/http://dx.doi.org/10.1016/j.fuel.2013.05.015

Krause E., Krzemień A., Smoliński A., 2015. *Analysis and assessment of a critical event during an underground coal gasification experiment*. Journal of Loss Prevention in the Process Industries **33**, 173-182. https://doi.org/10.1016/j.jlp.2014.12.014

Krzemień A., 2019. *Fire risk prevention in underground coal gasification (UCG) within active mines: Temperature forecast by means of MARS models*. Energy **170**, 777-790. https://doi.org/10.1016/j.energy.2018.12.179

Menéndez Álvarez M., Muñiz Sierra H., Sánchez Lasheras F., de Cos Juez F.J., 2017. *A parametric model of the LARCODEMS heavy media separator by means of multivariate adaptive regression splines*. Materials **10** (7). https://doi.org/10.3390/ma10070729

Milborrow S., 2017. *EARTH: Multivariate Adaptive Regression Splines.* R package, version 4.5.1.

Mocek P., Pieszczek M., Świadrowski J., Kapusta K., Wiatowski M., Stańczyk K., 2016. *Pilot-scale underground coal gasification (UCG) experiment in an operating Mine "Wieczorek" in Poland*. Energy **111**, 313-321. https://doi.org/10.1016/j.energy.2016.05.087

R Core Team., 2017. *R: A language and environment for statistical computing*. R Foundation for Statistical Computing, Vienna, Austria.

Sánchez Lasheras F., Vilán Vilán J., García Nieto P.J., del Coz Díaz J.J., 2010. *The use of design of experiments to improve a neural network model in order to predict the thickness of the chromium layer in a hard chromium plating process*. Mathematical and Computer Modelling **52** (7-8), 1169-1176. https://doi.org/10.1016/j.mcm.2010.03.007

Sekulic S., Kowalski B.R., 1992. *MARS: a tutorial*. Journal of Chemometrics **6**, 199-216.

Specht D.F., 1991. *A general regression neural network*. IEEE Transactions on Neural Networks **2** (6), 568-576. https://doi.org/10.1109/72.97934

Stańczyk K., Smoliński A., Kapusta K., Wiatowski M., Świdrowski J., Kotyrba A., Rogut J., 2010. *Dynamic experimental simulation of hydrogen oriented underground gasification of lignite*. Fuel **89** (11), 3307-3314. https://doi.org/10.1016/j.fuel.2010.03.004

Wang J., Wang Z., Xin L., Xu Z., Gui J., Lu X., 2017. *Temperature field distribution and parametric study in underground coal gasification stope.* International Journal of Thermal Sciences **111**, 66-77. https://doi.org/10.1016/j.ijthermalsci.2016.08.012

Wiatowski M., Kapusta K., Ludwik-Pardała M., Stańczyk K., 2016. *Ex-situ experimental simulation of hard coal underground gasification at elevated pressure*. Fuel **184**, 401-408. https://doi.org/10.1016/j.fuel.2016.07.020

Wiatowski M., Stańczyk K., Świądrowski J., Kapusta K., Cybulski K., Krause E., Smoliński A., 2012. *Semi-technical underground coal gasification (UCG) using the shaft method in Experimental Mine "Barbara"*. Fuel **99**, 170-179. https://doi.org/10.1016/j.fuel.2012.04.017

Zhu J., Wang C., Li C., Gao X., Zhao J., 2016. *Dynamic alarm prediction for critical alarms using a probabilistic model*. Chinese Journal of Chemical Engineering **24** (7), 881-885. https://doi.org/10.1016/j.cjche.2016.04.017